PERGAMON

Planetary and Space Science 48 (2000) 1437–1446

Planetary and Space Science

www.elsevier.nl/locate/planspasci

Impact cratering of granular mixture targets made of H_2O ice–CO_2 ice–pyrophylite

M. Arakawa[a,*], M. Higa[b], J. Leliwa-Kopystyński[c,d], N. Maeno[a]

[a] *Institute of Low Temperature Science, Hokkaido University, Kita-ku, Kita-19, Nishi-8, Sapporo 060-0819, Japan*
[b] *Institute of Space and Astronautical Science, Sagamihara 229, Japan*
[c] *Institute of Geophysics, University of Warsaw, ul. Pasteura 7, 02-093 Warsaw, Poland*
[d] *Space Research Center, Polish Academy of Sciences, ul. Bartycka 18A, 00-716 Warsaw, Poland*

Received 12 August 1999; received in revised form 6 March 2000; accepted 16 May 2000

Abstract

Experiments related to impacts onto three-component targets which could simulate cometary nucleus or planetary regolith cemented by ices are presented here. The impact velocities are from 133 to 632 m s^{-1}. The components are powdered mineral (pyrophylite), H_2O ice, and CO_2 ice mixed 1 : 1 : 0.74 by mass. The porosity of fresh samples is about 0.48. Two types of the samples were studied: nonheated samples and samples heated by thermal radiation. Within the samples a layered structure was formed. The cratering pattern strongly depended on the history of the samples. The craters formed in nonheated targets had regular shapes. The volume was easy to be determined and it was proportional to impact energy E. The crater depth scales as $E^{0.5}$. Impacts on the thermally stratified target led to ejection of a large amount of material from the loose sub-crustal layer. For some particular interval of impact velocity a cratering pattern can demonstrate unusual properties: small hole through the rigid crust and considerable mass transfer (radially, outward of the impact point) within sub-crustal layer.

1. Introduction

Impact events were very common in the Solar system in the remote past. Notwithstanding that the scale of the impacts and their frequency decreased dramatically with time, they are very typical at present as well. In any case, the studies of the impact events are of the first importance for understanding the evolution of Solar system bodies. The results of an impact recorded on a target surface can be very different. They depend mostly (i) on impactor energy and impactor momentum, (ii) on the physical properties of the target, and (iii) on gravity acceleration on the target surface. For the comprehensive discussion of the cratering phenomena see, for example, Melosh (1989) and the series of papers of Holsapple and Schmidt (1980, 1982, 1987). The latter are mostly dedicated to the discussion of scaling laws related to craters' dimensions. A special class of impacts important from the point of view of collisions of asteroids with cometary nuclei is studied by Kadono (1999). For this class the ratio (projectile density)/(target density) has a considerably higher value, 1–200.

To the authors of this paper no experiments related to cratering of layered, porous, and ices bearing medium are known. However, such a medium seems to be common in the uppermost layers of the cometary nuclei. It could also be related to the planetary regolith layer partially saturated by ices. The sandwich like structure, from top to bottom, is of the type: mineral crust, minerals plus less volatile ice (water ice), minerals plus water ice and other more volatile ices, pristine uniform material. Such a structure is possibly developed within the primitive medium forming a comet nucleus. It is expected that this structure is formed due to irradiation of initially uniform multi-component medium by the solar flux of energy. See, for example, the papers of Spohn and Benkhoff (1990, 1991) related to the series of KOSI experiments (KOSI is an acronym of German words KOmet SImulation) and, more recently, the papers of Kossacki et al. (1997, 1999). The numerical model of crater formation in a multi-layered structure bombarded by a meteoroid was recently considered by Jach et al. (1999a, b). The first of these papers is related to impacting of mineral and icy medium with voids; the second deals with impacting of Martian regolith assumed to be saturated by water ice. These numerical simulations showed that ice

* Corresponding author. Tel.: +81-11-706-7449; fax: +81-11-706-7142.

E-mail addresses: arak@lowtem.hokudai.ac.jp (M. Arakawa), jkopyst@mimuw.edu.pl (J. Leliwa-Kopystyński).

0032-0633/00/$ - see front matter
PII: S0032-0633(00)00088-X

Nomenclature

- m mass within the unit of volume V
- v projectile velocity
- V unit of volume
- α mass ratio of H_2O ice relative to rocky material "after mixing and compaction", and "before heating by radiation"
- β mass ratio of CO_2 ice relative to rocky material "after mixing and compaction", and "before heating by radiation"
- ε parameter determining how large fraction of the volume of voids is replenished by the resublimated H_2O or CO_2 ice; $0 \leqslant \varepsilon \leqslant 1$
- ρ density
- ψ porosity; $0 \leqslant \psi \leqslant 1$
- 0 a value of a parameter (in particular mass, density, and porosity) of a uniform three component sample in a state of initial conditions which are by definition: "after mixing and compaction", and "before heating by radiation"
- 1 a value of a parameter of the uniform two-component layer formed from water ice and rocky material (CO_2 ice has already sublimated)
- 2 a value of a parameter of the uniform one-component layer composed from rocky material only (CO_2 ice and H_2O ice have already sublimated)
- c CO_2 ice
- i H_2O ice
- r rocky material

surrounding the impact point could melt. The transformation from amorphous to crystalline ice could occur as well. The result strongly depends on the impact energy and momentum.

Water ice and minerals are undoubtedly the components of cometary nucleus. Carbon dioxide ice is one of the other ices, see e.g. Möhlman (1999) data related to comet 46P/Wirtanen. Carbon monoxide ice and ammonia ice are interesting as well. However, due to their low melting point and/or with their poisoning and corrosive properties they are difficult to be used for preparations of the samples/targets. After an impact the dispersed ejecta would be even more harmful. On the other hand, CO_2 ice is the easiest one after water ice to be used in the laboratory condition. Therefore, we have decided to operate with H_2O mixed with CO_2 ice.

2. Experiments

In this paper we deal with impact cratering of a finely granular medium which is the mixture of water ice, carbon dioxide ice, and mineral (pyrophylite). Due to the different pressure and temperature processing of the samples, we have received two different types of targets.

Preparation of the samples was made in a cold room ambient temperature equal to about -10°C. However, the fine powdered constituents were cooled in liquid nitrogen and then they were uniformly mixed with the initially required mass ratio $m_i : m_c : m_r = 1 : 1 : 1$. This mass ratio corresponds to the volume ratio $V_i : V_c : V_r = 3.015 : 1.780 : 1$. However, during preparation of the samples, escaping by sublimation of the most volatile component (CO_2 ice) was unavoidable. Weighing of the targets showed that the mass ratio of CO_2 ice diminished from an initial value 1 to 0.74 ± 0.05 on average. The mass ratio $H_2O/CO_2 = 1/0.74$ corresponds to molecular ratio $H_2O/CO_2 = 0.3$. It could not be far from real cometary composition. For example, for comet 46P/Wirtanen (a target of ROSETTA mission) it is plausible that contents by mass of water ice and of carbon dioxide ice are 40–60% and 2–30%, respectively (Möhlman, 1999). The content of mineral in the samples, 36% by mass, also fulfilled the cometary requirements.

The mixed medium, about 1.2 kg in total, was placed in a cylindrical container with diameter 16.6 cm and height 9.7 cm. The target container was constantly (until the shot) cooled by liquid nitrogen. The initial thickness of a sample was within the range from 7 to 9 cm. The porosity (a ratio of volume of the voids to the total volume) of the fresh sample was $\psi_0 = 0.479$, on average. After being placed in the container the sample was compacted at a pressure of 1.35×10^4 Pa during 15 min (Samples 07-1 to 08-3, further referred to as nonheated, NH, samples). The surface temperature of the piston used for compaction was within the range (205–240) K, see Fig. 1. The plots of temperature vs. time for NH samples (Fig. 1a) show that after compaction persisting only a few minutes the temperature on the surface and at the depth 4 cm reaches a slowly-changing state (the temperature behavior at the depth 4 cm in the sample 07-1 is an exception because of the uncertainty of its depth). Therefore, the samples from 08-4 to 10-3 (referred to as heated, H, samples) were compacted for 5 min. The thickness of each sample diminished to about 4 mm. The values of porosity of particular samples are listed in Table 1. In the following the samples of the series NH were ready to be impacted.

The samples of the series H were heated from the top by two infrared lamps with total power 200 W for 25 min. From the geometry of the lamps/sample system we estimated that about 0.2 of the total flux reached the surface of the sample. Therefore the incident flux was equal to about 2000 J m^{-2} s^{-1}. This value can be compared with the solar constant on the orbit of the Earth, C = 1360 J m^{-2} s^{-1}. Assuming low albedo of the material of the sample (at the first glance the albedo of the sample is mostly determined

Table 1
List of the impact experiments. The numbers in the parentheses are errors for an individual crater depth, diameter and volume, respectively

Shot no.	Surface heating	Projectile velocity v (m s^{-1})	Projectile energy E (J)	Porosity ψ_0	Crater depth[a] H (cm)	Crater diameter D (cm)	Crater volume V (cm^3)	Hole diameter (cm)
07–1	no	133	14.1	Not	0.6 (0.1)	3.5 (0.1)	2.71[b] (1.0)	Not appropriate
07–2	no	211	35.6	measured	1.4 (0.1)	6 (0.5)	7.58[b] (5.2)	for NH samples
07–3	no	288	65.9		2.1 (0.3)	6 (0.3)	19.4[b] (1.0)	
08–1	no	435	151	0.487	3.0 (0.2)	7.3 (0.3)	41.9[b] (8.3)	
08–2	no	531	224	0.472	3.1 (0.2)	7.3 (0.1)	41.5[b] (14.2)	
08–3	no	632	313	0.443	3.4 (0.2)	8.8 (0.2)	66.9[b] (12.1)	
08–4	yes	143	16.3	0.461	2.2 (0.1)	0[c]	0[d]	1.9 (0.3)
09–1	yes	208	34.2	0.524	4.0 (0.1)	7[c] (0.1)	12.0[d] (4.0)	2.3 (0.1)
10–1	yes	288[e]	66[e]	0.465	3.1 (0.2)	6[c] (0.4)	11.1[d] (4.5)	2.5 (0.1)
10–2	yes	536	228	0.498	3.6 (0.1)	6.5[c] (0.3)	14.4[d] (12.9)	Crust blown out
10–3	yes	455	161	0.476	3.0 (0.1)	5.2[c] (0.5)	20.4[d] (2.2)	Crust blown out

[a]Depth is measured from the actual surface of the sample in a moment of the shot.
[b]Volume excavated from layers (0′) and (0); it is equal to the total volume of a crater.
[c]Diameter is measured on the surface of layer (1).
[d]Volume excavated from layers (1) and (0); it is much less than the total volume of a crater.
[e]Values are estimated from typical our performance rather than measurements as described in the text. The uncertainty on v is ±10% and E is ±20%.

by the albedo of the mineral component, so it is equal to about 0.2 ± 0.1) the absorbed flux is only slightly less than the incident flux so the difference can be neglected. Therefore, the total absorbed energy is equal to about 6×10^4 J and this is an amount that is able to melt about 140 g of the cold H_2O ice, or to melt and then to evaporate about 20 g of this ice. These masses are equal to 1/3 or 1/20, respectively, of the total water ice content within the fresh sample.

The temperature was monitored on the sample surface as well as inside the sample, at a depth of about 4 cm, see Fig. 1. The temperature of the irradiated surface (Fig. 1b) increased to about 260 K during the first 5 min of irradiation, and then it increased slowly, approaching to 273 K after the next 20 min. Around the level 4 cm it slowly increased from about 185 K to about 200 K, therefore it remained near the sublimation temperature 195 K of the CO_2 ice.

As a result of heating the layered structure was formed. Such a structure was created due to the sublimation of volatiles: some of the vapor escaped out of the sample but some migrate inward and condensed on the deeper and cooler grains. Four layers can be distinguished in the heated samples. The layered structure was identified after the shot, by means of observation of the damage produced on the target by impactor. The best-defined layer is the uppermost crust. It is easy to be recognized in the central column of the Fig. 2. The two photos on the top of this column present the crust perforated by impactor and cracked radially. The structure of the crater is formed below the crust. Careful removal of the crust showed the crater in the center surrounded by the double-layer structure of subcrustal medium spreading on the pristine sample material. The two photos in the bottom of the central column illustrate the results of more energetic impacts: most of the crust and even most of near subcrustal layer was blown away. Observations of the post impact structures supported by the considerations related to sublimation of higher and lower volatile materials, CO_2 and H_2O ices respectively, allow to give the description of the structure of heated samples. From the bottom to the top (see the Appendix as well as Figs. 2 and 3) they are the following:

(0) Below the depth of about 4 cm (that corresponds to sublimation level of CO_2) the sample material remains unchanged, so it is a mixture of the three powdered materials previously densified by compression.
(1) In between about 4 and about 2.0–1.5 cm the material is quite well consolidated. We suppose that CO_2 ice has already sublimated from this layer. The consolidation is due to refreezing of the small amount of water vapor migrating inward in the sample from above. So, water ice originated from condensation of vapor cements together the grains of mineral and those of pristine ice.
(2) In between 2.0–1.5 and about 0.3 cm there is a loose dusty layer, almost free of ices. This layer remains too warm to keep CO_2 ice. Moreover, the layer preserved only a minor amount of water ice since the most of it has sublimated. Most of the vapor escapes from the sample but some of it condenses inward or upward, in the layer (1) or in the layer (1′), respectively.
(1′) The top layer, (0.3 ± 0.1) cm thick, consists of well consolidated dust and water ice. This layer is cemented by water ice of which some portion originates from condensation of vapor coming from the deeper region. During heating the flux of outgoing vapors is seen above the surface of the sample.

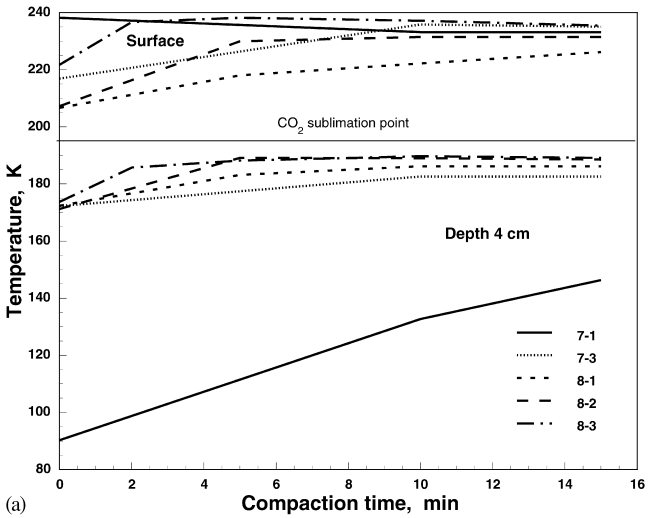

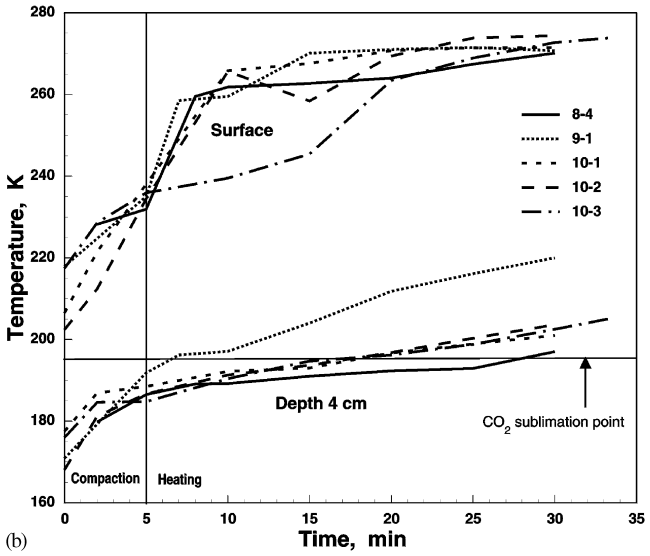

Fig. 1. Temperature vs. time on the surface of the samples and at a depth of 4 cm. (a) Samples 07-1 to 08-3 compacted for 15 min. (b) Samples 08-4 to 10-3 compacted for 5 min and next heated for 25 min by radiation.

Within the samples that were compressed but not heated by radiation, three layers are formed: A thin loose powder surface layer (brushed out before the shot); a hard layer denoted as (0′) where the medium is consolidated by resublimed CO_2; below the layer (0′), from a depth equal to 2 cm, the pristine layer (0) exists.

The sublimation, condensation, sintering, and transport processes in the icy/mineral media are considered in detail by Kossacki et al. (1997,1999). The first of these papers deals among the other things, with samples (denoted as S3) composed from the mixture of powders of mineral (dunite), of H_2O ice, and of CO_2 ice. The ratio of the constituents in S3 is 1 : 1 : 1 by volume, and thus it is similar to those used in the present work. However, some important differences between the sample S3 and the samples considered in this work must be noted. Firstly, in the present work a sample is heated in the ambient pressure whereas the S3 were heated in vacuum. Secondly, the time duration of thermal treatment in the experiments differs by more than an order of magnitude: heating in the present experiments was much shorter. Thirdly, the temperatures within the upper 4 cm of the samples in the present experiments were considerably higher than those observed in the S3. For the latter the formation of well-consolidated crust on the top was not observed: on the surface of S3 a layer of dust free-of-ice was formed. However, in the S3 a slightly consolidated layer consisted of mineral powder cemented by H_2O ice (analogous to the layer denoted as (1) in the present paper) has been formed below dusty layer.

The samples were impacted in a low-pressure ($< 10^4$ Pa) condition. More detailed specification of the pressure inside the target chamber was not possible. One must remember that the target was rather big and it continuously evaporated. There was a contradiction between a requirement of reaching of a pressure as low as possible and a requirement to perform a shot as quick as possible after putting a sample to the shot chamber. The cylindrical projectile made from water ice was accelerated vertically downward to the target surface by means of a vertical light-gas gun. The projectile diameter was 1.5 cm and its mass was 1.6 g. The gun was installed in the cold room (-10°C) at the Institute of Low Temperature Science, Hokkaido University at Sapporo (Japan); for a description of the gun see Kato et al. (1995). The impact velocity was measured by means of a standard method of recording the flight time difference of projectile between two laser beams using a digitizing oscilloscope. The accuracy was better than 5%, therefore the impact energy was measured with an error bar less than $\pm 10\%$. The impact velocities were from 142 to 632 m s^{-1}. The choice of the upper value is limited by the target size: for higher velocities the cratering pattern would be disturbed by the presence of the edge of the target container.

Immediately after a shot the sample was taken out of the impact chamber and the geometrical and physical properties of the crater were investigated.

3. Results

Fig. 2 presents the craters produced in the both types of targets: nonirradiated targets (left column) compared with irradiated targets (central and right columns). Each horizontal pair of the craters was produced by identical projectiles with similar velocity, therefore similar energy. The differences between craters of one pair are clearly visible. The craters formed in nonheated targets have morphology similar to that typically observed in the laboratories when uniform media were impacted by projectiles with velocity of the order of several hundreds meters per second (e.g. Schmidt and Housen (1987), Melosh (1989), Kato et al. (1995)). In that case a crater bowl, sometimes with a central pit surrounded

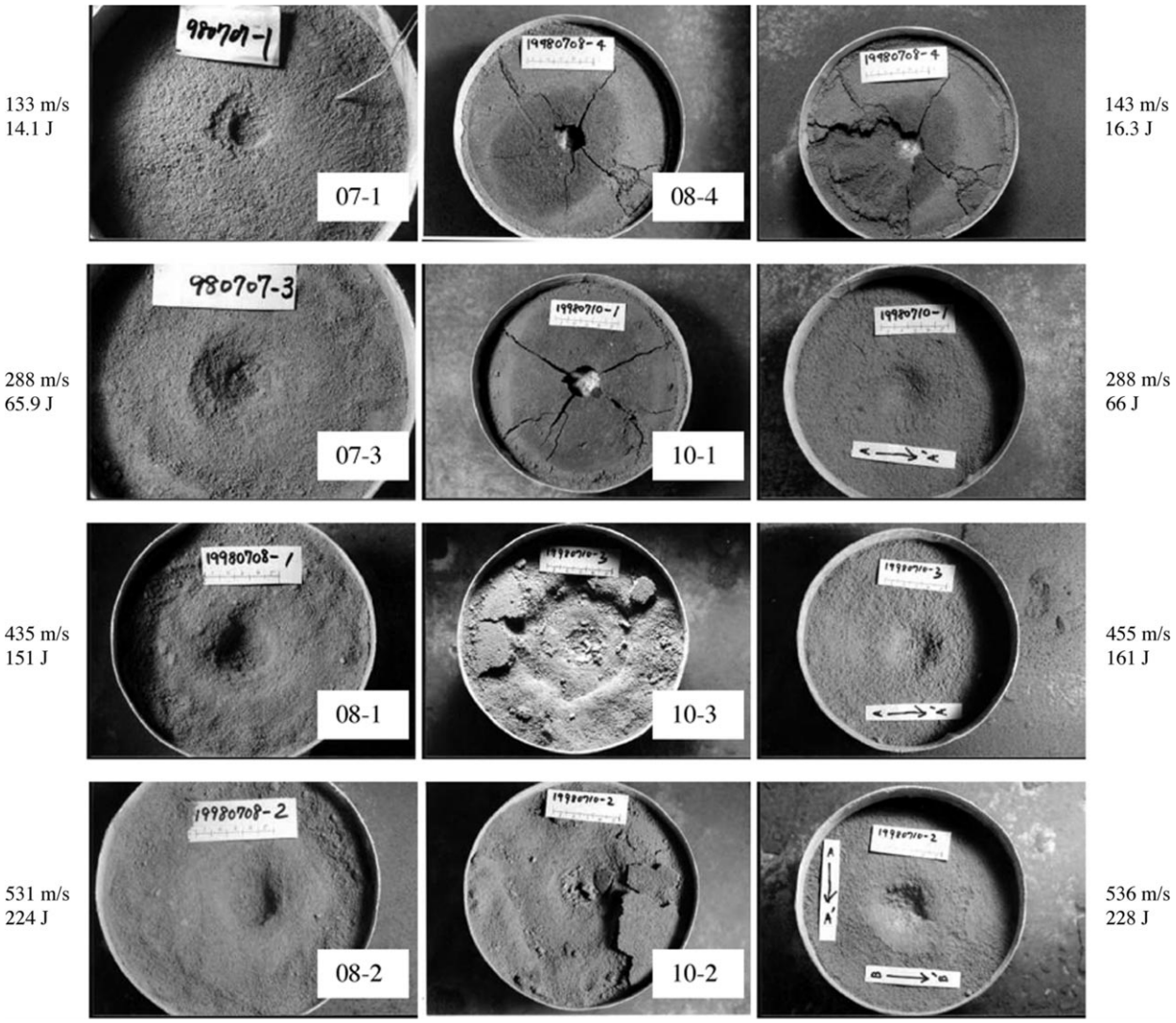

Fig. 2. The craters produced in the nonirradiated targets (left column) and irradiated targets (central and right columns). Left column: view of the craters after brushing out a thin dust layer. Central column: view of the crater immediately after the shot. Right column: view of the crater after removal of a thin crust and after brushing out a highly porous layer below it. Each horizontally presented pair of craters 07-1 and 08-4, 07-3 and 10-1, 08-1 and 10-3 corresponds to similar impact velocity and therefore to similar impact energy, see Table 1. In the case of low velocity impact (targets 08-4 and 10-1) the ejecta from the crater are caught by the crust: see the case 08-4 (top right) where the structure of a crater rim below the crust appears. For higher-impact velocity (target 10-3) almost the whole crust is ejected out of the target container.

by a terrace, was formed. In the cases of the heated samples the picture is quite different. The heating produced stratification of the samples. In particular, their uppermost layer (the crust) has higher strength and higher density than the material laying immediately below.

In the case of heated targets the crater is produced below the rigid and brittle crust. If the velocity of impactor v is not high enough (in our case $v = 143$, 208, and 288 m s^{-1}) the impactor pierces the crust producing a hole and the surrounding radial cracks. For higher velocity ($v = 455$ and 536 m s^{-1}) the crust is fragmented and the fragments are blown away exposing the crater formed on the deeper layers of a target. One can expect, that for larger container (in the case of half-infinite flat target) the impact would have produced a bowl-shaped crater surrounded by the relatively large shallow terrace (being a result of blowing away of the weak layer (2)).

Let us apply the formulae given in the Appendix, for calculation of porosity and density in the different layers of the irradiated samples (series 2), see Table 2 and Fig. 4. The following values of the bulk densities of the constituents are adopted for porosity and density calculations: for H_2O ice $\rho_i = 922$ kg m^{-3}, for CO_2 ice $\rho_c = 1562$ kg m^{-3}, and for pyrophylite $\rho_r = 2780$ kg m^{-3}. The initial (before heating) mass ratios of the components are $m_r : m_i : m_c = 1 : 1 : 0.74$, and therefore $\alpha = 1$ and

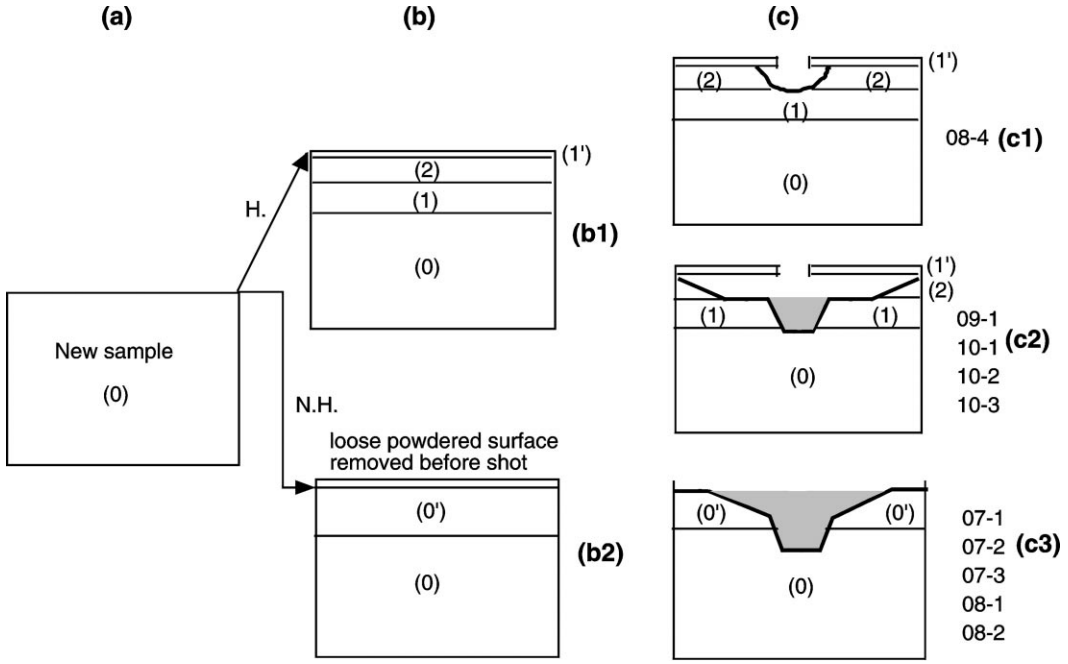

Fig. 3. Schematic vertical cross section of the samples. *H* denotes 5 min of compaction plus 25 min of radiative heating. NH denotes that 15 min of compaction was applied. The craters' profiles are marked by heavy lines. The calculated volumes are shadowed. (a) Uniform new sample ready to be compressed (series 1) or to be compressed and heated by radiation from the top (series 2). (b1) The sample stratified by radiative heating. The consecutive layers, from bottom to top, are (0) Pristine uniform mixture, (1) mineral and H_2O ice layer, (2) mineral high porous layer without CO_2 ice, and (1′) mineral and H_2O ice layer without CO_2 ice, enriched in H_2O ice. In reality, each layer passes continuously to the next one, when the depth changes. (b2) In case when 15 min of compaction was applied, the thin layer composed of mineral and water ice powders (CO_2 ice has sublimated) is created on the sample surface. This layer is brushed out before the shot. Below the powder layer another well consolidated layer denoted as (0′) is formed. We believe that it is cemented by resublimated CO_2 which in the gaseous form migrates upward and inward from the top layer. Therefore, the composition of the layer (0′) can be written schematically: (0′) = (0) + (CO_2 ice). (c1, c2) The heated stratified samples cratered by a lower velocity impact (c1), and by a higher velocity impact (c2). (c3) The sample of the type (b2) after cratering. In reality, the uppermost layer is depleted in CO_2 ice due to its sublimation. The structure of the sample material near the surface is similar to the intermediate structure between layer (1) and (0) of case (b).

Table 2
The porosities and densities of the different layers of "idealized" samples after radiative heating. Porosity of a fresh, not heated sample and the porosity corresponding to percolation threshold are assumed to be equal $\psi_0 = 0.479 \pm 0.025$, and $\psi_1' = \psi_0' = 0.1$, respectively. The porosities ψ_1, ψ_2, the densities $\rho_0, \rho_1, \rho_2, \rho_1', \rho_0'$ and the replenish factors $\varepsilon_i, \varepsilon_c$ are calculated from fomulae (A.3), (A.6)–(A.13). Note very high porosity and very low density of the ice-free layer (2). On the other hand, thin surface layer (1′) as well as layer (0′) are of low porosity and high density

Porosity and density	Uniform sample (before heating) (0)	Layer without CO_2 ice (1)	Layer without CO_2 ice and without H_2O ice (2)	Layer without CO_2 ice and enriched in H_2O ice (1′)	Uniform sample enriched in CO_2 ice (0′)
ψ	0.479 ± 0.025	0.608 ± 0.028	0.902 ± 0.082	0.1 therefore $\varepsilon_i = 0.836 \pm 0.008$	0.1 therefore $\varepsilon_c = 0.791 \pm 0.011$
ρ (kg m^{-3})	744 ± 64	543 ± 36	272 ± 18	1011 ± 62	1336 ± 103

$\beta = 0.74$. The average initial porosity of the samples (therefore the porosity of the layer (0)) is $\psi_0 = 0.479 \pm 0.025$. The last column of Table 2 deals with the condensation of water ice within the pores: pristine pores as well as these formed after CO_2 sublimation can be replenished by H_2O ice. The lowest possible porosity ψ_1' of the layer (1) corresponds to the percolation threshold in this layer. In our case this is an unknown and nonmeasurable value. However, an assumption $\psi_1' = 0.1$ seems to be physically reasonable. Anyway, for any values from an interval (0, 0.2) the threshold porosity ψ_1' has no major influence on the density of the hypothetical, water saturated layer (1′) given in Table 2. This value corresponds to the pore replenishing factor $\varepsilon_i = 0.836 \pm 0.008$ and the density $\rho_1' = (1012 \pm 62)$ kg m^{-3}. Note that the density ρ_1' calculated for percolation threshold is the maximum possible density of the material forming the fine grained mineral and water ice crust.

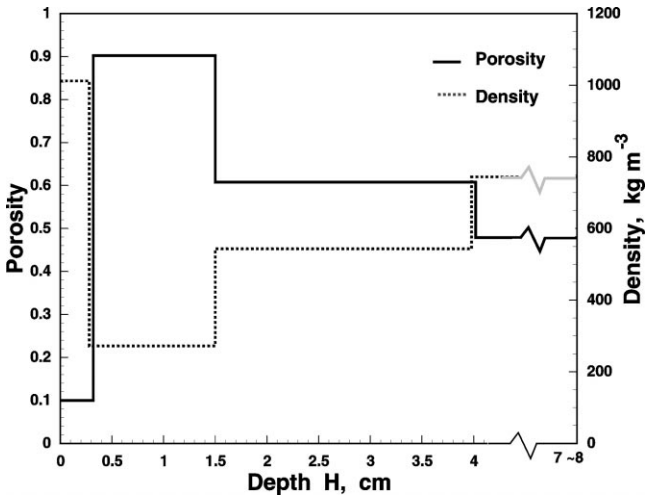

Fig. 4. Porosity and density in the different layers of the heated samples, see Table 2.

The measurements of the vertical cross section of a crater, see Fig. 5, is a common work for the impact experiments. In our case, the profiles of the craters produced on nonheated targets were defined from the surface to the bottom of the crater pit. However, the shapes of the craters produced on heated targets are very complicated, mostly because the target container is too small. The flat sub-surface structure of a crater spreads out to the wall of the container and interacts with it.

In Fig. 6, the crater volume V vs. impact energy E (see Table 1) is presented. The volumes are calculated by means of using the average profiles of the craters with assumed axial symmetry. Fig. 7 presents crater depth H vs. E. Both the figures illustrate data for nonheated as well as for heated samples.

The volume V of the craters produced in nonheated targets, their diameter D measured on the surface, and their depth H below the surface, change with impactor energy (for 14.1 J $< E <$ 313 J) as follows:

$$V = (0.216 \pm 0.019)E, \quad (1)$$

$$D = 2.04E^{0.253}, \qquad r = 0.942, \quad (2)$$

$$H = 0.176E^{0.543}, \qquad r = 0.966. \quad (3)$$

Here, and in the following formulae V is in cm^3, D and H are in cm, and E is in J; r is the correlation coefficient. An assumption that crater volume V scales as D^2H leads, via relations (2) and (3), to proportionality $V \propto E^{1.049}$ which is very closed to $V \propto E$ expressed by Eq. (1). Therefore, the scaling assumption is reasonable and it leads to the conclusion that crater shape remains unchanged (for the impacts within the energy interval applied in the experiments). A stronger assumption that crater shape is conical, $V = \pi D^2 H/12$, gives $V = 0.182E^{1.049}$ which is similar (within an error bar) to Eq. (1).

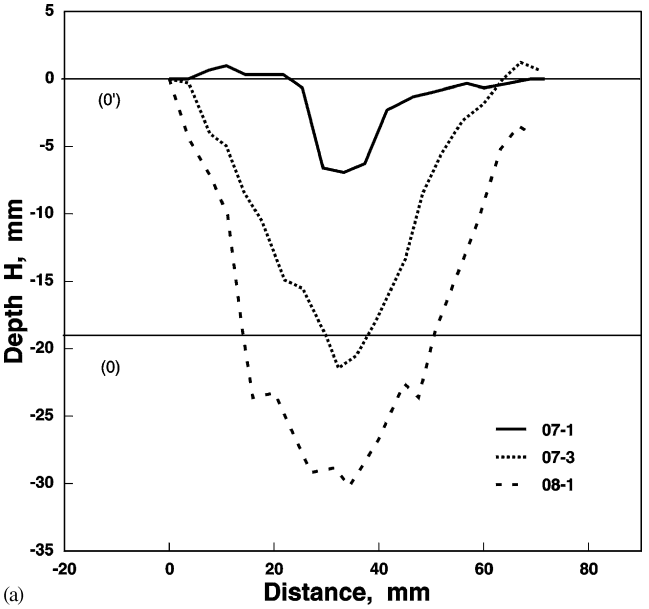

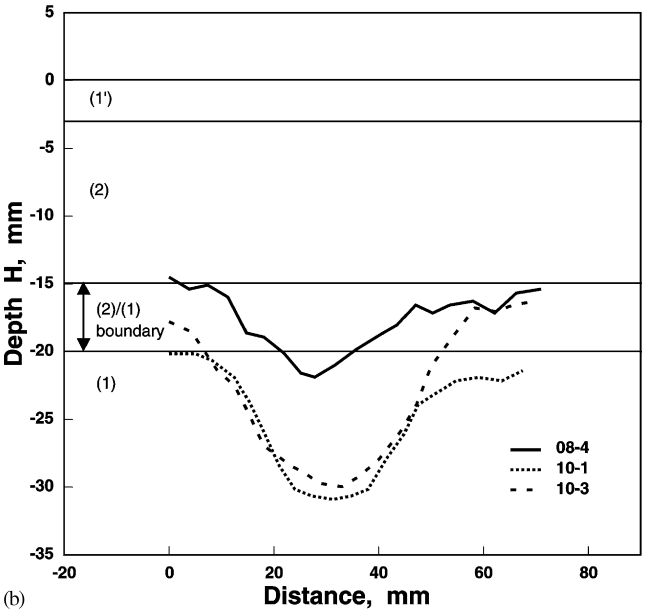

Fig. 5. Vertical cross section of some craters. The six, most axially symmetric craters' profiles are presented here. (a) Nonheated targets 07-1, 07-3, and 08-1 produced by impactors with energy 14.1, 165.9 and 151 J, respectively. Profiles related to the craters are formed within the layers (0) and (0′). (b) Heated target 08-4, 10-1, and 10-3 produced by impactors with energy 16.3, ≈ 65 and 161 J, respectively. The actual profiles of the craters are related to layer (1). Above this layer the most of the material of layer (2) was radially transported under the quite well preserved crust (1′), shot 08-4 and 10-1. For higher energy, shot 10-3 the most of layer (2) as well as the crust (1′) were blown away.

Craters formed in the heated targets are more complicated. For impactor energy applied in our experiments, 16.3 J $< E <$ 228 J, the prevailing part of the volume of the crater is excavated from the highly porous layer (2) (see Fig. 3 c1, c2). The craters can be divided into two classes depending on impactor energy:

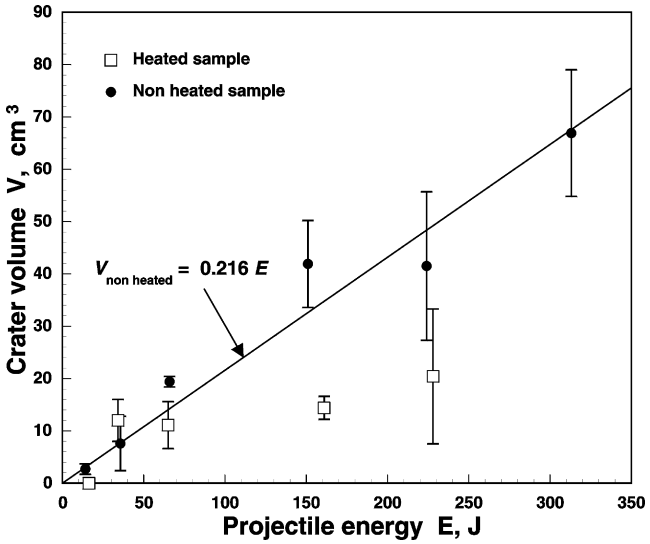

Fig. 6. Crater volume vs. projectile energy.

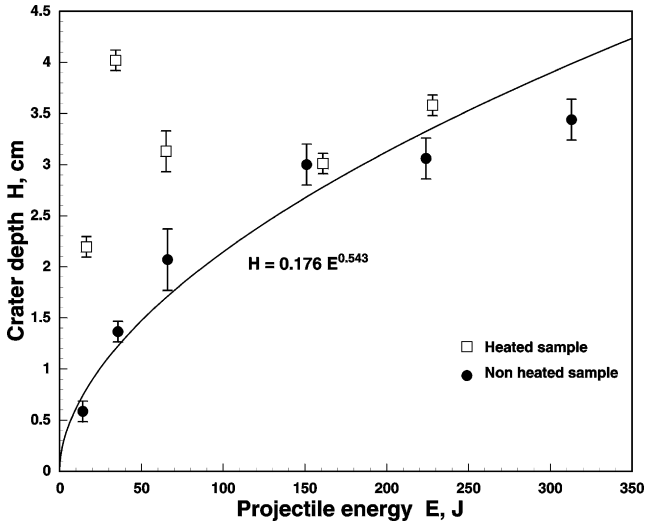

Fig. 7. Crater depth vs. projectile energy.

(1) Subcrustal craters are formed by low energy of an impactor. It penetrates through the top layer (layer (1′) or crust) producing an entrance hole (see Fig. 3 c1, c2). The diameter of this hole is equal about 1.5 times diameter of impactor, see the two photographs in the central column on Fig. 2 and the data in Table 1. The ejecta are blown away radially under the layer (1′). Since the energy of ejecta is not high enough, the crust is not destroyed.

(2) Craters with more typical morphology are formed if the energy of impactor is large enough to blow out the crust. However, the layered structure of the target significantly influences the structure of a crater which has a terrace shape.

The geometrical parameters characterizing the craters, specially their diameters and volumes are more difficult to be fitted to impactor energy than it was for parameters of the craters formed on nonheated targets. An impact 08-4 with energy 16.3 J has not produced any cavity on the layer (1). For higher energies of impactors (4 shots with energies $34.2, \approx 66, 161$, and 228 J) we have found that the crater depth, cavity diameter measured on the surface of the layer (1), and the volume of this cavity excavated from the layers (1) and (0) are, in practice, energy independent:

$$H = (3.4 \pm 0.5)\ \text{cm}, \qquad D = (6.2 \pm 0.8)\ \text{cm},$$
$$V = (14 \pm 4)\ \text{cm}^3. \tag{4}$$

Measurement of crater diameter on the target's surface was impossible: for low impactor's energy it was just a hole in the crust (shots 08-4, 09-1, 10-1); for high energy the destruction of the crust was so strong that it spread out to the walls of the sample container (shots 10-2 and 10-3).

In general, heating of the targets involves their stratification leading to depth-dependent density and strength distributions. A crater on the heated target is bigger and flatter in comparison to the crater produced in the nonheated target (if impact energy is the same).

4. Applications for planetology and conclusions

Any kind of attempts of extrapolation of laboratory experiments onto planetary scale of events must be performed with a special caution. However, in some cases a vast extrapolation is not necessary and the almost direct interpretation is possible. In our case, the impact energy is of the order of 10 or 100 J. These values correspond to impactors with masses of the order of (0.1–0.01) g hitting the targets with velocities of the order of (1–10) km s^{-1}. The latter are the reasonable encounter velocities in the outer solar system or in the satellite systems. Let us consider a new comet arriving from the Oort cloud to the inner solar system or any other icy-mineral body residing in the outer planetary system. In both cases the solar radiation can produce a stratified sub-surface structure. The composition and the thickness of the particular layers will depend on the contents of different ices and on the temperature distribution beneath the surface.

In our case the most interesting conclusion is probably related to the formation of craters on the stratified medium. According to the experiments there exists a range of energy of the impactor for which the craters are formed below the icy-cemented mineral crust. The crust itself remains almost intact except where it is perforated by the projectile. Applying this observation to the large ensemble of the craters we can conclude that the crater record observed from above the surface (from above the crust) will be seriously different from what would appear after removing the crust.

It is worth comparing the present experimental results with others performed by taking into account volume, diameter and depth of craters vs. impact energy E. In this work, for nonheated samples prepared from powdered materials, Eqs. (1)–(3) were fitted. For the samples made from the icy blocks the excavation is an order of magnitude less efficient. Indeed, for cratering of a CO_2-ice block Burchell et al. (1998) fit the following relations

$$V = 0.035E^{1.13}, \quad D = 0.95E^{0.38},$$
$$H = 0.178E^{0.40}, \ 1\ \text{J} < E < 400\ \text{J}. \tag{5}$$

In the paper of Burchell et al. (1998) a list of results related to cratering of H_2O-ice blocks obtained by different authors is also given. The power law formulae $y = aE^b$ ($y = V$, or D, or H; a, b are the numerical coefficients) are fitted. Compared to similar impacts (impacts with similar energy) in H_2O-ice blocks, the craters in CO_2-ice blocks are smaller by a factor 2.2 in diameter and 8.9 in volume. Craters described in this work (Eqs. (1)–(3)) are larger than the CO_2 craters of Burchell et al. (1998) but slightly smaller (at 100 J) than the ice on ice (H_2O) craters of Kato et al. (1995).

Let us perform some geometrical considerations. The volume of a spherical segment with height H and diameter D given by Eqs. (2) and (3) is equal to $V_{\text{sph.seg.}} = 0.29E^{1.049}(1 + E^{0.037})$. This is a relation close to Eq. (1), $V = 0.216E$, for crater volume of nonheated target (this work). The volume of a cone with height H and diameter D given by Eqs. (5) is $V_{\text{cone}} = 0.042E^{1.16}$ and this is very similar to crater volume $V = 0.035E^{1.13}$ in CO_2 block.

There exists some analogy between our impacts into heated targets and the impacts into low density material studied by Kadono, 1999. He considers a hypervelocity impact of high-density projectile (an asteroid) on low-density target (a comet). However, his target is uniform, not layered the like heated targets in this work. The result of Kadono's impact can be described by a carrot-(spindle) shaped cavity. Its maximum diameter is larger than the entrance hole diameter. Therefore, to some extent, the cavity of Kadono consists of a similar structure to our craters in layered heated samples.

Acknowledgements

The authors greatly appreciate the kindness of anonymous reviewers for their very detailed study of the manuscript which allows to introduce important improvements. J. Leliwa-Kopystyński would like to express his thanks to Prof. Norikazu Maeno from the Institute of Low Temperature Science, Hokkaido University at Sapporo, for his enthusiastic acceptation of the proposed work as well as for a research grant.

Appendix

Formulae for density and porosity

The following possibilities of different layers of the sample are considered the most typical ones:

(0) *Uniform* (*initial*) *three-component sample*. The unit of volume occupied by rock, by H_2O ice, by CO_2 ice, and by voids is equal to

$$V = V_r + V_i + V_c + \psi_0 V \tag{A.1}$$

and the total mass in the unit of volume is equal to

$$m_0 = m_r + m_i + m_c = (1 + \alpha + \beta)m_r. \tag{A.2}$$

Therefore the relations between the density ρ_0 of a sample, its volume V, and its porosity ψ_0, are

$$\rho_0 = (1 + \alpha + \beta)m_r/V = (1 + \alpha + \beta)(1 - \psi_0)\zeta, \tag{A.3}$$

$$\psi_0 = 1 - \frac{m_r}{\zeta V}, \tag{A.4}$$

where

$$\frac{1}{\zeta} = \frac{1}{\rho_r} + \frac{\alpha}{\rho_i} + \frac{\beta}{\rho_c}. \tag{A.5}$$

(1) *Uniform two-component layer*: the whole CO_2 ice has sublimated leaving the volume V_c empty. Let us assume that no other transformations have occurred. Therefore the density and the porosity of this layer are equal to

$$\rho_1 = (1 + \alpha)m_r/V = (1 + \alpha)(1 - \psi_0)\zeta, \tag{A.6}$$

$$\psi_1 = \psi_0 + V_c/V = \psi_0 + (1 - \psi_0)\beta\zeta/\rho_c. \tag{A.7}$$

(2) *Uniform one-component mineral layer*: CO_2 and H_2O have sublimated leaving the volume V_c and V_i empty. Density and porosity of this layer are equal to

$$\rho_2 = m_r/V = (1 - \psi_0)\zeta, \tag{A.8}$$

$$\psi_2 = \psi_1 + \frac{V_i}{V} = \psi_0 + (1 - \psi_0)\left(\frac{\alpha}{\rho_i} + \frac{\beta}{\rho_c}\right)\zeta. \tag{A.9}$$

Cases (0)–(2) are the simplest and idealized ones. However, the uppermost layer of a sample heated by radiation has the modified structure, that can be modeled as follows:

(1′) *Uniform two-component layer*: the whole CO_2 ice has sublimated leaving the volume V_c empty and then in some part of the volume of the voids water ice is condensed. Therefore the total volume of the pores after sublimation of CO_2 is equal to $\psi_1 V = (\psi_0 V + V_c)$, see case (1). Let us assume that a fraction ε_i of this volume is occupied by migrating water vapor that has resublimed within the pores. (For models related to migration/condensation see Kossacki et al., 1997, 1999.) The density and the porosity of these modified mineral plus water ice layer enriched with extra water ice are equal to

$$\rho_1' = (m_r + m_i + \varepsilon_i\psi_1 V\rho_i)/V = \rho_1 + \varepsilon\psi_1\rho_i, \tag{A.10}$$

$$\psi_1' = (1 - \varepsilon_i)\psi_1. \tag{A.11}$$

(0′) This is the layer (0) enriched in CO_2 coming from the top in gaseous form and condensing within the pores. In this case the density and the porosity are

$$\rho_0' = (m_r + m_i + m_c + \varepsilon_c \psi_0 V \rho_c)/V = \rho_0 + \varepsilon_c \psi_0 \rho_c, \quad (A.12)$$

$$\psi_0' = (1 - \varepsilon_c)\psi_0. \quad (A.13)$$

Here ε_c has the similar meaning like ε_i for case (1′).

References

Burchell, M.J., Brooke-Thomas, W., Leliwa-Kopystyński, J., Zarnecki, J.C., 1998. Hypervelocity impact experiments on solid CO_2 targets. Icarus 131, 210–222.

Holsapple, K.A., Schmidt, R.M., 1980. On the scaling of crater dimensions. 1. Explosive processes. J. Geophys. Res. 85 (B12), 7247–7255.

Holsapple, K.A., Schmidt, R.M., 1982. On the scaling of crater dimensions. 2. Impact processes. J. Geophys. Res. 87 (B3), 1849–1870.

Holsapple, K.A., Schmidt, R.M., 1987. Point source solutions and coupling parameters in cratering mechanics. J. Geophys. Res. 92 (B7), 6350–6376.

Jach, K., Kortas, Ł., Leliwa-Kopystyński, J., Morka, M., Mroczkowski, M., Panowicz, R., Świerczyński, R., Wolanski, P., 1999a. Cratering of comet nucleus by meteoroids. Adv. Space Res. 23, 1319–1323.

Jach, K., Leliwa-Kopystyński, J., Morka, A., Mroczkowski, M., Panowicz, R., Świerczyński, R., Wolanski, P., 1999b. Modifications of martian ice-saturated regolith due to meteoroid impact. Adv. Space Res. 23, 1933–1937.

Kadono, T., 1999. Hypervelocity impact into low density material and cometary outburst. Planet. Space Sci. 47, 305–318.

Kato, M., Iijima, Y., Arakawa, M., Okimura, Y., Fujimura, A., Maeno, N., Mizutani, H., 1995. Ice on ice impact experiments. Icarus 113, 423–441.

Kossacki, K.J., Kömle, N.I., Leliwa-Kopystyński, J., Kargl, G., 1997. Laboratory investigation of the evolution of cometary analogs: results and interpretation. Icarus 128, 127–144.

Kossacki, K.J., Szutowicz, S., Leliwa-Kopystynski, J., 1999. Comet 46P/Wirtanen: evolution of the subsurface layer. Icarus 142, 202–218.

Melosh, H.J., 1989. Impact Cratering. Oxford University Press, Oxford.

Möhlman, D., 1999. 46 P/Wirtanen Nucleus (Fact Sheets: Rosetta Nucleus Modeling Group), ESA, SP-1165.

Schmidt, R.M., Housen, K.R., 1987. Some recent advances in the scaling of impact and explosion cratering. Int. J. Impact Engng. 5, 543–560.

Spohn, T., Benkhoff, J., 1990. Thermal history models for KOSI sublimation experiments. Icarus 87, 358–371.

Spohn, T., Benkhoff, J., 1991. Thermal history of the KOSI samples. Geophys. Res. Lett. 18, 261–264.